INVESTIGATION OF THE AIR "SPARK" PRODUCED BY FOCUSED LASER RADIATION. III

V. V. KOROBKIN, S. L. MANDEL'SHTAM, P. P. PASHININ, A. V. PROKHINDEEV, A. M. PROKHOROV, N. K. SUKHODREV, and M. Ya. SHCHELEV

P. N. Lebedev Physics Institute, Academy of Sciences, U.S.S.R.

Submitted February 20, 1967

Zh. Eksp. Teor. Fiz. 53, 116—123 (July, 1967)

The development of a laser spark in air during the action of the laser radiation pulse is investigated. The velocity of the luminous spark front towards the focusing lens is measured simultaneously by means of an image converter and on basis of the Doppler shift of the reflected laser light frequency. It is found that immediately after appearance of the spark the maximal velocity of the luminous front is $\sim 4.5 \times 10^7$ cm/sec, whereas the velocity derived from the Doppler shift is $\sim 1.10^7$ cm/sec. The dependence of the two velocities on the flux density of the laser radiation is derived. The ion temperature is determined ($\sim 6 \times 10^5$ °K) on the basis of the velocity of radial motion of the spark plasma and it is found to be approximately equal to the electron temperature of the plasma. The structure of the spark plasma in the region of the focus is studied with an image converter and by a shadow photography technique. On the basis of the data obtained it is concluded that forward motion of the ionization region towards the lens is the result of successive breakdowns at separate points and subsequent hydrodynamic movement from each such point after the breakdown.

1. INTRODUCTION

MUCH attention has been paid recently to investigations of sparks produced by focusing laser radiation in gases. Greatest interest attaches to the initial stages of the laser spark, prior to the termination of the laser pulse, since the specific features of this phenomenon, connected with the presence of a powerful light-wave field, become manifest here. It has been established that during this stage the ionization region moves in towards lens, opposite to the laser beam direction, with a speed $\sim 10^7$ cm/sec, and the plasma has an electron temperature ~ 100 eV and an initial electron density $\sim 10^{19}$—10^{20} cm^{-3} [1,3-5]. On the basis of the obtained experimental data, different mechanisms were proposed for the motion of the plasma ionization front towards the focusing lens [1,2,6]. However, the relative roles of these mechanisms are not yet fully clear at the present. The velocities obtained by different methods differ greatly in magnitude and their variation during the time of the laser emission has different characters [1-7-9]. In addition, there are no experimental data on the ion temperature of the laser spark.

We present here the results of experiments on the dynamics of spark development during the initial stage, on the structure of the plasma near the focus, and on measurements of the ion temperature of the laser spark, and we propose a possible mechanism whereby the ionization region moves towards the focusing lens; this mechanism agrees with the available experimental data.

2. INVESTIGATION OF THE MOTION OF THE SPARK FRONT

To clarify the mechanism of the longitudinal spark development, we measured the propagation velocity of the ionization region towards the focusing lens simultaneously by two methods: by determining the Doppler frequency shift of the laser emission scattered by the leading front of the spark, and by time-scanning the image of the spark with an electron-optical converter (EOC) The experimental setup is shown in Fig. 1.

A Q-switched ruby laser produced a pulse of average power ~ 100 MW at a duration at half-height ~ 15 nsec. The Q-switching was with the aid of a Pockels cell with a KDP crystal. The laser radiation was focused by a lens L of focal length F = 50 mm, as a result of which breakdown occurred in the air and the so called laser spark was produced.

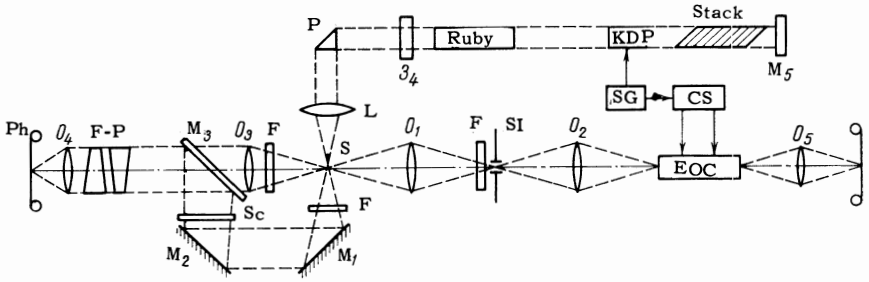

FIG. 1. Diagram of experiment for the measurement of the speeds of development of the laser spark. L – lens, S – spark, EOC – electron-optical converter, CS – control system, SG – spark generator, M_1–M_5 – mirrors, O_1–O_5 – objectives, Sl – slit, F – light filters, FP – Fabry-Perot interferometer, Sc – scatterer, Ph – photographic film.

To obtain the time sweep of the motion of the luminous front of the spark in the longitudinal direction, the spark image was produced with an objective O_1 on the slit S1 oriented along the spark. The slit in turn was projected on the photocathode of the EOC with the aid of objective O_2. The image is swept on the EOC screen in a direction perpendicular to the screen. The minimum EOC sweep duration was 100 nsec; the time resolution, determined experimentally, amounted to 0.5 nsec under these conditions. The EOC control circuit was triggered [10] with the aid of a spark generator, which simultaneously served also to control the electrooptic shutter of the laser Q-switch. Filters F placed ahead of the slit S1 made it possible to obtain streak photographs in different regions of the spectrum. In addition, it was possible to obtain with this scheme streak photographs in reflected light of the laser beam itself. In this case, no slit is necessary, since the transverse dimension of the spark front producing the reflection is very small, amounting to 0.1–0.2 mm.

We used a Fabry-Perot interferometer to measure the Doppler frequency shift of the laser emission scattered by the leading front of the spark. The distance between the interferometer mirrors was 0.6 mm, and the dispersion region was 4.1 Å. The installation of the interferometer is clear from Fig. 1. Objectives O_3 and O_4, located at their focal distances from the spark and from the plane of the film Ph, respectively, produce the image of the spark in this plane. Simultaneously, an image of the Fabry-Perot interferometer, placed between the objectives, is produced in the Ph plane, and the exposure of each element of the individual interference ring is produced by the laser emission scattered by the corresponding section of the spark. The rings corresponding to the positions of the unshifted frequency are obtained on account of the part of the laser emission passing beyond the focus prior to the instant of the breakdown. This is effected by the system of mirrors M_1, M_2, M_3 and the scatterer Sc. It is obvious that such a scheme makes it possible to register the Doppler frequency shift of the laser radiation scattered at different points of the spark near the focus of the lens L.

A streak photograph of the spark obtained with the EOC in reflected light is shown in Fig. 2a. The photograph of the spark obtained simultaneously through the Fabry-Perot interferometer is shown in Fig. 2b. It is seen from these photographs that the motion of the spark front is intermittent: after the breakdown occurs, the spark front moves towards the lens continuously only over an average path length of about 0.3 mm; breakdown is then produced at the next point, located closer to the lens at distances on the order of 0.3–0.5 mm from the front, etc. The presence of a spark structure of this type and the time variation of the intensity of the scattered light were already noted earlier [1,11]. The photographs of Fig. 2 can be used to plot the variation of the spark velocity, measured by these two methods, as a function of the distance from the front to the initial point of breakdown occurrence. A typical plot is shown in Fig. 3. We call attention to the fact that the velocities measured by the two methods greatly differ in magnitude and have different time variations. At the very start of the spark, the velocity obtained with the EOC reaches 4×10^7 cm/sec, whereas the Doppler shift gives a value 1×10^7 cm/sec. As the spark develops, the speeds differ less and less and both speeds coincide at approximately the last third of the spark.

To explain the spark-developed mechanism, we investigated the dependence of the front velocity on the laser emission flux density J. To determine J, it is necessary to know the laser radiation power P observed in the plasma at each instant of time, and the cross section area of the spark S at the corresponding instant. To measure these quantities, the experimental setup shown in Fig. 1 was modified somewhat. The radiation power absorbed by the plasma was measured by determining the difference of the oscillograms of

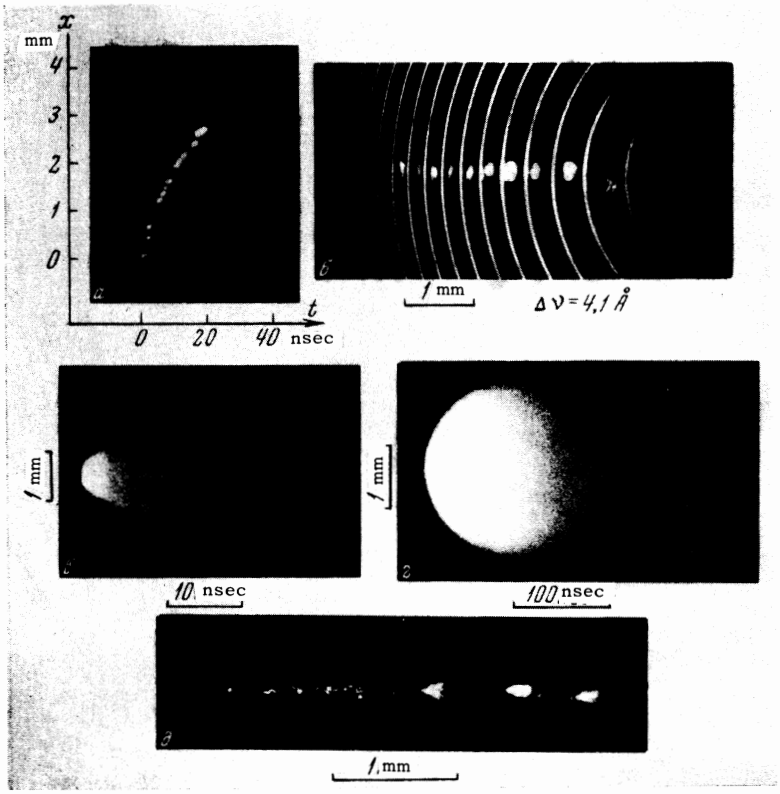

FIG. 2. a – Time sweep, obtained with EOC, of the motion of the laser spark towards the lens. The photograph was obtained in reflected laser light. b – Doppler shift of the laser radiation reflected from the spark. The interferometer dispersion region is 4.1 A. c, d – transverse spreading of spark plasma. e – photograph of spark in reflected laser light.

two pulses, one incident and the other passing beyond the focal region of the lens L. We used in the experiments a calibrated coaxial photocell and a high speed oscilloscope (S1-10). The resolving power of the registration system was 1 nsec. To measure the transverse dimension, the spectrum was photographed on film with a micro-objective having 10x magnification. The photography was in reflected laser light. Since the reflection occurred only from the leading front, it is possible to determine from such a photograph the area of the cross section of the leading front of the spark at each point. The area of the cross section of the spark front at different instants of time can then be determined from the known position of the front at each instant of time and from the photographs obtained simultaneously with the EOC.

The experiments have shown that the power P absorbed in the spark changes from the start to the end of the spark by approximately 10—12 times, and the average flux density by approximately 6—8 times. The speed of the ionization region, determined from the time sweep on the EOC, changes in this case by approximately one order of magnitude, and the speed measured from the Doppler shift changes by 1.5—2 times (Fig. 3). A detailed analysis of the dependence of the speeds on J is given in Sec. 5.

3. INVESTIGATION OF THE TRANSVERSE SPREADING OF THE SPARK PLASMA[1)]

The expansion of the gas heated in the front of the spark in a plane perpendicular to the laser beam leads to the formation of a shock wave that diverges radially from the zone of the light channel. The speed of this radial shock wave is of the order of the speed of sound in the hot gas [6], and is consequently determined by the temperature of the spark plasma. This makes it possible to measure the plasma ion temperature.

To photograph the transverse motion of the plasma, the EOC and the slit shown in Fig. 1 were turned 90° so that the objective O_1 produced an image of the spark perpendicular to the slot. The photography was through neutral filters, so that the photographs show also the laser light reflected on the leading front as its image passes through the slit, as well as the glow produced by the radially expanding plasma itself. It is seen from the photographs of Fig. 2c that the transverse spreading begins immediately after the passage of the leading front of the spark.

The maximum speed of transverse spreading, obtained in these experiments, is 6×10^6 cm/sec.

[1)] S. I. Fedotov took part in the experiments on the measurement of the speeds of the longitudinal and transverse development of the spark with the aid of the EOP.

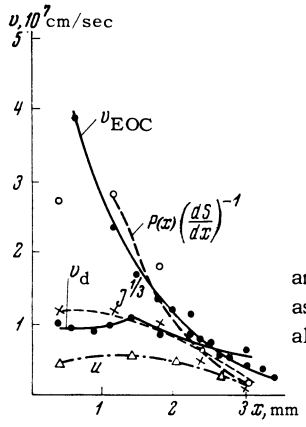

FIG. 3. Longitudinal speeds v_d and v_{EOC} and transverse speed u as functions of the coordinate x along the spark.

The most intense glow from the spark continues for approximately 150 nsec after the breakdown (Fig. 2d).

We investigated the variation of the transverse speed as a function of the distance to the point of initial breakdown. We found that the transverse speed is practically the same at different points. As a rule, at the very start of the spark, the transverse speed is somewhat smaller, $\sim 4.5 \times 10^6$ cm/sec. Then, with increasing distance from the breakdown point, the speed increases quite rapidly to 6×10^6 cm/sec, and again drops off towards the end of the spark to $3-4 \times 10^6$ cm/sec. The dependence of the transverse speed on the distance to the initial-breakdown point is shown in Fig. 3, together with plots for the longitudinal speeds.

4. INVESTIGATION OF THE SPARK STRUCTURE

To investigate the spark structure during the time of action of the laser pulse, we obtained shadow photographs of the region near the focus of the lens by transmitted laser light. In this experiment, we used a ruby laser Q-switched by a rotating prism. The laser pulse duration at half-height was 30 nsec at an average power 70—80 MW.

The optical setup is shown in Fig. 4. The laser radiation is focused by lens L_1. Breakdown is

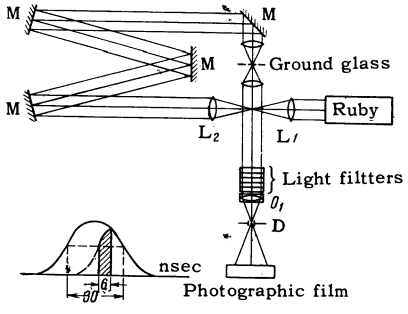

FIG. 4. Diagram of experiment for the investigation of the spark structure.

produced in the focal region and the resultant plasma begins to absorb the light strongly, so that only the front part of the laser pulse passes beyond the focal region [11]. The use of a liquid saturable filter, which becomes transparent when a definite light-pulse power level is reached, has made it possible to cut off also the initial part of the transmitted pulse. As a result, the duration of the pulse shaped in this manner was 5—6 nsec. This shortened laser light pulse was collimated then by lens L_2 and used to illuminate the spark. A system of lenses and mirrors, together with ground glass, ensured uniformity of the illuminating field and made it possible to regulate the delay of the illuminating pulse relative to the instant of occurrence of breakdown, within an interval 6—40 nsec.

Shadow photographs with ~6 nsec exposure were obtained with a "Tessar" lens of 5x magnification on photographic film sensitive to the red light. A small diaphragm, with 2 mm diameter, was placed in the focus of the lens; this diaphragm did not attenuate the illuminating pulse, but greatly reduced the intensity of the radiation incident on the photographic plate from the spark itself. The same purpose was served by red filters KS-17 and KS-19. With such a scheme, the radiation from the spark itself was completely suppressed, but it was impossible to get rid of the laser light scattered by the front of the spark.

Figure 5a shows a typical shadow photograph of the spark, obtained by this method 17 nsec after the start of the breakdown. We call attention to the fact that the region near the focus has a complicated structure, containing sections of greatly differing transparency to the laser light. This picture apparently proves that there is no stationary motion of the leading front towards the lens in the spark during the time of laser emission, and that the breakdown takes place successively at different points, whose distance from the focal region increases continuously. The opaque regions correspond then to regions with high plasma density, while the bright bands correspond to rarefaction waves occurring on the trailing edge of the detonation wave. We note that in the last section of the spark, the structure as a rule vanishes, that is, the plasma fills the entire region of the spark. The light points, which are clearly seen in the center of the photograph, are due to scattering of the laser radiation by the leading front of the spark. A photograph obtained 150 nsec after the start of the spark, shows the collision of the shock waves emerging from two sparks (Fig. 5b).

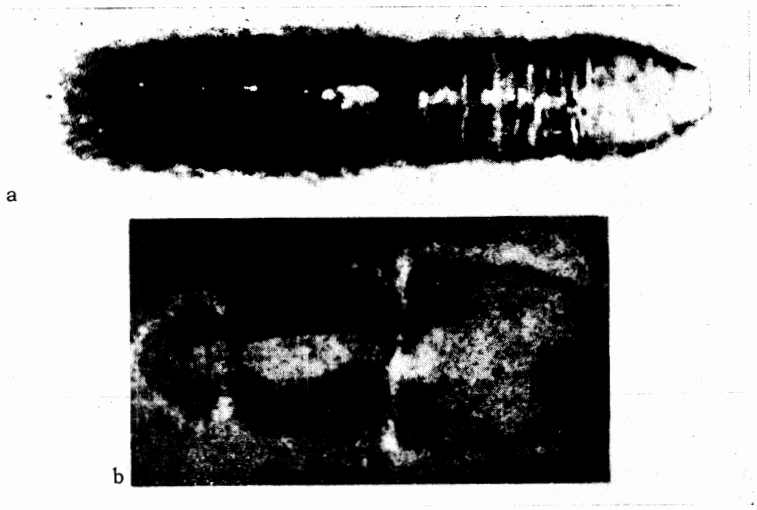

FIG. 5. a – shadow photograph of the spark 17 nsec after the breakdown; b – shadow photograph of the spark 150 nsec after the breakdown. Collision of two shock waves emerging from different parts of the spark is observed.

5. DISCUSSION OF RESULTS

The experimental results obtained in this paper, namely the difference between the velocities measured by the two methods, and the presence of a distinct spark-plasma structure, revealed both by the EOC and by the shadow photographs, make it possible to construct the following picture of spark development: When the front of the light wave reaches a definite threshold value, breakdown occurs in the focal point, with rapid heating of the plasma to ~50—100 eV; this produces a detonation wave moving towards the lens. The motion continues until breakdown takes place in a second point, located closer to the lens, and here again a detonation wave is produced, etc. The time interval between successive breakdowns is approximately 3 nsec. During that time the front, moving at 10^7 cm/sec, advances a distance of 0.3 mm. This stage of front motion can apparently be quite well described by the hydrodynamic mechanism, and the speed determined from the Doppler shift is that of the detonation wave. Indeed, in the case of the hydrodynamic mechanism of plasma development, the speed of the detonation wave v_d is

$$v_d = [(\gamma^2 - 1)(\gamma + 1)\varepsilon / \gamma]^{1/2}, \quad (1)$$

where γ is the effective adiabatic exponent and ϵ is the specific energy of the plasma. On the other hand, the transverse spreading speed is equal to the speed of sound in the hot plasma

$$u = \sqrt{\gamma(\gamma - 1)\varepsilon} \approx v_d/2. \quad (2)$$

This is precisely the relation between u and v_d observed in our experiments.

In addition, the experimentally-obtained dependence of v_d on the flux density absorbed in the wave also coincides with the theoretical dependence for the hydrodynamic mechanism (Fig. 3):

$$v_d = [2(\gamma^2 - 1)J/\rho_0]^{1/3}. \quad (3)$$

Using the measured transverse spreading speed we can calculate from (2) the specific plasma energy ϵ and determine the ion temperature T_i. According to Raĭzer [6], for air of normal density in the temperature region 5×10^5—10^6 °K we have

$$\varepsilon = 4.5 \cdot 10^{13} (T_i/5 \cdot 10^5)^{7/4} \text{ erg/g},$$

whence

$$T_i = 1.25 \cdot 10^{-2} (u)^{8/7} \text{°K}, \quad (4)$$

giving $T_i = 5 \times 10^5$ °K for $u = 4.5 \times 10^6$ cm/sec and $T_i = 7 \times 10^5$ °K for $u = 6 \times 10^6$ cm/sec.

The same values of the temperature are obtained from estimates of the average power absorbed in the spark. The volume of the spark, calculated from the photograph of the spark in reflected light (Fig. 2e), is 6×10^{-5} cm^3. Assuming an air density $\rho_0 = 1.3 \times 10^{-3}$ g/cm^3 and knowing the energy absorbed in the spark (0.6 J), we obtain a specific energy 7.8×10^{13} erg/g and $T_i \approx 6.8 \times 10^5$ °K.

The numerical value of the plasma ion temperature T_i, calculated from (4) using the measured transverse spreading velocity. coincides with the value of the electron temperature T_e determined in [1] from the intensity of the x-radiation of the spark. This confirms theoretical estimates according to which the deviation between the electron and ion temperature of the plasma should not be large under these conditions. Indeed, in a strong high-frequency field E, the ratio of the electron to ion temperature is given by

$$T_e/T_i = 1 + (E/E_p)^2, \quad (5)$$

where E_p is the magnitude of the plasma field:

$$E_p^2 = 3km\delta T_i(\omega^2 + \nu_{eff}^2) / e^2,$$

δ is the coefficient of energy transfer per collision, and ν_{eff} is the effective collision frequency.

Under our conditions $\delta \approx 10^{-3}$ and $E_p \approx 10^5$ cgs esu, whereas $E \approx 3 \times 10^4$ cgs esu. Substituting these values of E and E_p in (5), we obtain $T_e/T_i \approx 1.1$, that is, under the conditions of our experiment the electron temperature can exceed the ion temperature by not more than 10%.

The total motion of the spark front, consisting of breakdowns at successive points and hydrodynamic motion from each point after the breakdowns, gives the ionization-region speed registered by the EOC. This speed is much higher than the speed of the hydrodynamic wave near the focus, as can be seen from the plots of Fig. 3.

As is well known, the breakdown condition is written in the form

$$\int_0^t J(x,\tau)\,d\tau = \int_0^t \frac{P(\tau)}{S(x)}\,d\tau = C, \qquad (6)$$

where $P(\tau)$ is the power absorbed in the spark, S(x) the area of the transverse cross section of the beam at each point along the beam, and C is a constant. Equation (6) gives the dependence of the position of the front on the time x(t). Differentiating this expression with respect to t, we obtain the expression for the speed of the successive breakdown

$$v_{br} = \frac{dx}{dt} = \frac{P[t(x)]}{CdS/dx}. \qquad (7)$$

Figure 3 shows a plot of $P(x)(dS/dx)^{-1}$ against the coordinate x. The value of P(x) was obtained from oscillograms, which gave P(t), and from the EOC time sweeps, which gave x(t); the values of dS/dx were calculated from the photographs of the spark in reflected light. It is seen from the plot that the agreement between the speeds calculated from (7) and those directly measured with the EOC is satisfactory. We note that for, constant dS/dx the speed is directly proportional to the power absorbed in the spark. In our measurements, the assumption that dS/dx is constant is valid for the greater part of the spark.

Let us consider now the possible causes of the appearance of breakdowns at discrete points spaced ~0.3 mm apart. Inasmuch as the initial breakdown produces a plasma with temperature $\sim(6\text{—}7) \times 10^5$ °K, a radiation wave with a speed greatly exceeding that of the detonation wave will propagate from the breakdown point. The plasma radiation will heat the adjacent layer of the air almost instantaneously, and this heating will occur at the distance equal to the average mean free path of the radiation in the cold gas. For 100-eV photons, which make up the bulk of the radiation in such a plasma, this amounts to ~0.1—10 mm. Observation of such a rapidly produced photoionization aureole around the spark was reported in [12]. The surrounding gas will be heated by this radiation to a temperature 1—3 eV, in agreement with the previously noted [2,3] small width of the Doppler-scattering line. It is perfectly natural for laser-beam propagation conditions to be much different in such a plasma than in the initial unheated gas.

In particular, at such a temperature, the plasma becomes opaque to the laser emission; under these conditions, the radiation mean free path for a ruby-laser quantum is $\sim 10^{-2}$ mm. Therefore the region of intense absorption should shift towards the laser by an amount equal to the heating zone, and the laser beam is always "cut off" near the leading front of the radiation wave. If the breakdown conditions are satisfied at that point by that time, then breakdown takes place in the vicinity of the leading front of the radiation wave, producing in turn a new focus for a high temperature plasma, serving as a source of a radiation and a detonation wave. This mechanism explains qualitatively the intermittent character of the breakdowns.

In principle, the appearance of discrete breakdown points can have also another cause, namely self trapping of the beam, which, according to Askar'yan [13] and Litvak [14], should take place in the produced plasma. It will also shift the breakdown region towards the lens. However, self-trapping of the beam has never been observed in a plasma experimentally. The question of the mechanism of formation of discrete breakdown points is being investigated by us at present in greater detail.

In conclusion, the authors are deeply grateful to G. A. Askar'yan and Yu. P. Raĭzer for fruitful discussions, to M. M. Butslov for useful recommendations on the use of the electron optical converter, and to V. A. Shamburov for supplying a KDP crystal for Q-switching.

[1] S. L. Mandel'shtam, P. P. Pashinin, A. M. Prokhorov, Yu. P. Raĭzer, and N. K. Sukhodrev, Zh. Eksp. Teor. Fiz. 49, 127 (1965) [Sov. Phys.-JETP 22, 91 (1966).

[2]S. A. Ramsden and P. Savic, Nature **203**, 1217 (1964).

[3]A. J. Alcock, P. P. Pashinin, and S. A. Ramsden, Phys. Rev. Lett. **17**, 528 (1966).

[4]A. J. Alcock and S. A. Ramsden, Appl. Phys. Lett. **8**, 187 (1966).

[5]A. Kakos, G. V. Ostrovskaya, Yu. J. Ostrovskii, and A. N. Zaidel, Phys. Lett. **23**, 81 (1966).

[6]Yu. P. Raĭzer, Zh. Eksp. Teor. Fiz. **48**, 1508 (1965) [Sov. Phys.-JETP **21**, 1009 (1965)].

[7]R. V. Ambartsumyan, N. G. Basov, V. A. Boĭko, V. S. Zuev, O. N. Krokhin, P. G. Kryukov, Yu. V. Senatskiĭ, and Yu. Yu. Stoĭlov, ibid. **48**, 1583 (1965) [**21**, 1061 (1965)].

[8]F. Floux and P. Veyrie, Compt. rend. **261**, 3771 (1965).

[9]S. A. Ramsden and W. E. Davies, Phys. Rev. Lett. **13**, 227 (1965).

[10]V. V. Korobkin, L. P. Malyavkin, and M. Ya. Shchelev, PTÉ No. 4, 129 (1965).

[11]S. L. Mandelstam, P. P. Pashinin, A. M. Prokhorov, and N. K. Sukhodrev, Proc. of the Int. Conf. on Physics of Quantum Electronics, N. Y. (1966).

[12]G. A. Askar'yan, M. S. Rabinovich, M. M. Savchenko, A. D. Smirnova, V. B. Studenov, ZhETF Pis. Red. **1**, No. 6, 18 (1965) [JETP Lett. **1**, 162 (1965)]. G. A. Askar'yan, M. S. Rabinovich, M. M. Savchenko, and V. K. Stepanov, ibid. **3**, 465 (1966) [**3**, 303 (1966)].

[13]G. A. Askar'yan, Zh. Eksp. Teor. Fiz. **42**, 1567 (1962) Soviet Phys.-JETP **15**, 1088 (1962)].

[14]A. G. Litvak, Izv. VUZov Radiofizika **9**, 675 (1966).

Translated by J. G. Adashko
14